

Characterization of the Zinc Binding Site in Methionine Synthase Enzymes of *Escherichia coli*: The Role of Zinc in the Methylation of Homocysteine

Katrina Peariso,[‡] Celia W. Goulding,[§] Sha Huang,[§] Rowena G. Matthews,^{*,§} and James E. Penner-Hahn^{*,‡}

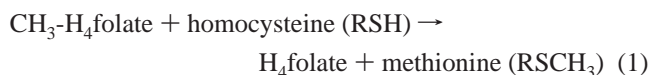
Contribution from the Department of Chemistry, the Biophysics Research Division, and the Department of Biological Chemistry, The University of Michigan, Ann Arbor, Michigan 48109-1055

Received February 20, 1998

Abstract: X-ray absorption spectroscopy, using the analytical methodology described in the previous paper, has been used to determine the ligation of the essential zinc ions in cobalamin-dependent (MetH) and cobalamin-independent (MetE) methionine synthases from *Escherichia coli* and to probe directly the changes in zinc ligation that occur upon addition of the thiol substrate, homocysteine, to each enzyme. Extended X-ray absorption fine structure (EXAFS) spectra of native MetE and a truncated fragment of MetH containing the substrate-binding sites are consistent with ZnS₂(N/O)₂ and ZnS₃(N/O) ligation, respectively. Previous mutagenesis studies of the homocysteine binding region of MetH had identified two putative thiolate zinc ligands, Cys310 and Cys311. Since the EXAFS spectra indicate that the zinc is coordinated to three sulfur ligands derived from the protein, a third conserved cysteine, Cys247, was mutated to alanine, resulting in a MetH fragment that binds only 0.09 equiv of zinc per mol of protein and exhibits no methylcobalamin-homocysteine methyltransferase activity. Upon addition of L-homocysteine, the X-ray absorption near edge structure changes for both enzymes, and the EXAFS spectra show changes consistent with the coordination of a sulfur, giving a ZnS₃(N/O) site for MetE and a ZnS₄ site for MetH. Only the L-homocysteine enantiomer causes these effects; the addition of D-homocysteine to MetH(2-649) gives no detectable changes in the EXAFS or the near edge regions. These results are consistent with a mechanism in which the homocysteine is ligated to zinc. Homocysteine is then able to initiate nucleophilic attack on the methyl group needed for methionine formation, with the methyl group bound either to methylcobalamin in MetH or to a polyglutamate derivative of methyltetrahydrofolate in MetE.

Zinc has long been recognized as an important cofactor in biological molecules, either as a structural template in protein folding or as a Lewis acid catalyst that can readily adopt 4-, 5-, or 6-coordination.¹ Recent reports have suggested that zinc is able to play a catalytic role in the activation of thiols as nucleophiles at physiological pH.^{2–4} In the present paper, we use the methodology described in the accompanying paper⁵ to characterize the zinc binding sites of two newly identified zinc-containing enzymes, cobalamin-dependent and cobalamin-independent methionine synthase,^{6,7} and to probe the changes in zinc ligation that occur upon addition of homocysteine to each of these enzymes.

Cells of *Escherichia coli* possess two separate enzymes for the biosynthesis of methionine, cobalamin-dependent (MetH) and cobalamin-independent (MetE) methionine synthase.⁸ Both enzymes catalyze the transfer of a methyl group from methyltetrahydrofolate (CH₃-H₄folate) to homocysteine for the production of the amino acid methionine (eq 1).



MetH is a 1227 residue protein that requires a cobalamin cofactor, an electron donor, and S-adenosylmethionine⁹ for activity.^{8,10} The first 353 residues of methionine synthase have been shown to be responsible for homocysteine binding and activation.¹¹ During primary turnover, the methyl group is displaced from the CH₃-H₄folate by nucleophilic attack of the cob(I)alamin cofactor and then transferred from methylcobalamin to the homocysteine thiol. High-resolution crystal structures of the 27 kDa cobalamin binding region (residues 650–

(8) Foster, M. A.; Tejerina, G.; Guest, J. R.; Woods, D. D. *Biochem. J.* **1964**, *92*, 476–488.

(9) Abbreviations: AdoMet, S-adenosylmethionine; Hcy, L-homocysteine; H₄folate, 5,6,7,8-tetrahydrofolate; CH₃-H₄folate, 5-methyltetrahydrofolate; Tris, tris(hydroxymethyl)aminomethane.

(10) Mangum, J. H.; Scrimgeour, K. G. *Fed. Proc.* **1962**, *21*, 242.

(11) Goulding, C. W.; Postigo, D.; Matthews, R. G. *Biochemistry* **1997**, *36*, 8082–8091.

* To whom correspondence should be addressed.

[‡] Department of Chemistry.

[§] Biophysics Research Division and the Department of Biological Chemistry.

(1) Vallee, B. L.; Auld, D. S. *Acc. Chem. Res.* **1993**, *26*, 543–551.

(2) Matthews, R. G.; Goulding, C. W. *Curr. Opin. Chem. Biol.* **1997**, *1*, 332–339.

(3) Wilker, J. J.; Lippard, S. J. *Inorg. Chem.* **1997**, *36*, 969–978.

(4) Myers, L. C.; Terranova, M. P.; Ferentz, A. E.; Wagner, G.; Verdine, G. L. *Science* **1993**, *261*, 1164–1167.

(5) Clark-Baldwin, K.; Tierney, D. L.; Govindaswamy, N.; Gruff, E. S.; Kim, C.; Berg, J.; Koch, S. A.; Penner-Hahn, J. E. *J. Am. Chem. Soc.* **1998**, *120*, 8401–8409.

(6) Gonzalez, J. C.; Peariso, K.; Penner-Hahn, J. E.; Matthews, R. G. *Biochemistry* **1996**, *35*, 12228–12234.

(7) Goulding, C. W.; Matthews, R. G. *Biochemistry* **1997**, *36*, 15749–15757.

896)¹² and the 38 kDa C-terminal AdoMet binding domain (residues 897–1227)¹³ have been solved, but a structure is not yet available for the remaining N-terminal 71 kDa region responsible for binding CH₃-H₄folate and homocysteine. An N-terminal fragment of wild-type MetH containing the substrate-binding sites, MetH(2–649), catalyzes methyl transfer from exogenous methylcobalamin to homocysteine to yield cob(II)-alamin and methionine with a second-order rate constant of 2320 M⁻¹ s⁻¹. Methyl transfer from methyltetrahydrofolate to exogenous cob(I)alamin is also catalyzed by the fragment, with a second-order rate constant of 594 M⁻¹ s⁻¹.¹¹

In contrast to MetH, comparatively little is known about the structure and turnover mechanism of MetE. MetE is an 85 kDa enzyme that requires a polyglutamate derivative of methyltetrahydrofolate for enzymatic activity. Its activity is stimulated by phosphate and by divalent cations such as Mg²⁺ and Mn²⁺.^{14,15} There is no detectable sequence similarity between MetH and MetE. MetE does not require a cobalamin cofactor and is homologous to the methionine synthase enzymes isolated from the plant species *Catharanthus roseus*¹⁶ and *Oryza sativa*.¹⁷ Due to the absence of vitamin B₁₂ in the plant kingdom, MetE-type enzymes are the only known catalysts for the production of methionine in these organisms.¹⁶

Despite a lack of sequence similarity and the differences in cofactor requirements, recent work by Matthews and colleagues has shown that zinc is required for catalytic activity of both methionine synthase enzymes.^{6,7} Wild-type MetH(2-1227) and the truncated fragment MetH(2-649) each contain 1 equiv of zinc.⁷ The zinc site within MetH has not previously been fully characterized. However, within the first 353 residues of *E. coli* MetH that comprise the homocysteine-binding region are three cysteines (Cys247, Cys310, and Cys311) that are conserved in the sequences of cobalamin-dependent methionine synthase from *Escherichia coli*,^{18–20} *Mycobacterium leprae*,²¹ *Synechocystis sp.*,²² *Caenorhabditis elegans*,²³ and *Homo sapiens*.^{24–26} The vicinal cysteines, Cys310 and Cys311, are candidate ligands for the zinc site in MetH. Mutation of either Cys310 or Cys311 to either alanine or serine causes the activity of the mutant holoenzymes to decrease to background levels and the methylcobalamin prosthetic group is not demethylated in the presence of homocysteine.⁷ Similarly, the Cys310Ala and Cys311Ala MetH(2-649) mutant proteins do not catalyze methyl transfer

from exogenous methylcobalamin to homocysteine. None of the purified mutant proteins contain zinc.¹¹ In contrast to the dramatic effect of these mutations on methyl transfer from methylcobalamin to homocysteine, these mutations do not affect methyltetrahydrofolate-cob(I)alamin methyltransferase activity.

Cobalamin-independent methionine synthase also requires zinc for catalytic activity;⁶ one of the conserved cysteine residues in MetE is a candidate ligand. Mutation of Cys726 to serine in MetE leads to loss of bound zinc and of all detectable enzymatic activity.⁶ Cys726 is conserved in the amino acid sequences of cobalamin-independent methionine synthase from *Catharanthus roseus*,¹⁶ *Haemophilus influenzae*,²⁷ *Methanobacterium thermoautotrophicum*,²⁸ *Oryza sativa*,¹⁷ and *Saccharomyces cerevisiae*.²⁹ Also conserved in these alignments is a His-X-Cys motif, His⁶⁴¹-Met-Cys⁶⁴³ in the *E. coli* MetE sequence. When MetE is treated with [¹⁴C]iodoacetamide, Cys726 is preferentially labeled, but a second minor peak corresponding to the tryptic peptide containing this His-Met-Cys motif is also seen on HPLC chromatograms of tryptic digests of the labeled enzyme.¹⁵ His641, Cys643, and Cys726 are the only histidine and cysteine residues conserved between bacteria, plants, and archaea.

To determine the details of the zinc ligation in MetE and MetH and to probe the role of zinc in the methylation of homocysteine, we have used EXAFS and XANES to characterize the zinc ligation in both MetE and MetH before and after addition of substrate. In addition, since our EXAFS studies suggest that three sulfur ligands are contributed to zinc by the MetH protein, we have used site-directed mutagenesis of Cys247 to alanine to identify this cysteine as a third candidate amino acid zinc ligand.

Materials and Methods

Materials. The GeneClean Kit was purchased from Bio 101. Vent polymerase and T4 DNA ligase were purchased from New England Biolabs. Restriction enzymes were obtained from Promega and New England Biolabs. The Sequenase Version 2.0 DNA sequencing kit was purchased from United States Biochemical. All primers were made at the University of Michigan Protein and Carbohydrate Structure Facility. (6*R,S*)-H₄folate and (6*R,S*)-CH₃-H₄folate (calcium salt) were purchased from Dr. B. Schircks Laboratories (Jona, Switzerland). ¹⁴C-(6*R,S*)-CH₃-H₄folate was purchased from Amersham. TiCl₃ in 2 M HCl was obtained from Aldrich. L-Homocysteine thiolactone, hydroxocobalamin, AdoMet, methylcobalamin, and dicyanocobinamide were purchased from Sigma. AG1-X8 resin, Chelex 100 resin, and protein dye reagent were purchased from Bio-Rad.

Construction of a Truncated methH Gene for the Mutant Cys247Ala. Mutation Cys247Ala was constructed in MetH(2-649) with use of overlap extension PCR,³⁰ where the cysteine247 codon (TGT) in the *methH* gene was changed to alanine (GCT). For construction of each mutation, four oligonucleotide primers were used: the sequence of primer A is identical to residues 613–628 of the noncoding strand of the published *methH* sequence and begins 334 nt³¹ upstream of the first nucleotide of the cysteine247 codon; primer D is complementary to residues 1443–1466 of the noncoding strand of the *methH* gene, 479 nt downstream of the first nucleotide of the cysteine247 codon; primer B is complementary to nt 953–973 of the noncoding strand, with the exception of the changes at nt 962 and 963 to convert the cysteine codon to one specifying alanine; the sequence of primer C is identical

(12) Drennan, C. L.; Huang, S.; Drummond, J. T.; Matthews, R. G.; Ludwig, M. L. *Science* **1994**, *266*, 1669–1674.

(13) Dixon, M.; Huang, S.; Matthews, R. G.; Ludwig, M. L. *Structure* **1996**, *4*, 1263–1275.

(14) Whitfield, C. D.; Steers, E. J., Jr.; Weissbach, H. J. *Biol. Chem.* **1970**, *245*, 390–401.

(15) Gonzalez, J. C.; Banerjee, R. V.; Huang, S.; Sumner, J. S.; Matthews, R. G. *Biochemistry* **1992**, *31*, 6045–6056.

(16) Eichel, J.; Gonzalez, J. C.; Hotze, M.; Matthews, R. G.; Schroeder, J. *Eur. J. Biochem.* **1995**, *230*, 1053–1058.

(17) Sasaki, T.; Miyao, A.; Yamamoto, K. GenBank Accession No. D40225, 1994.

(18) Banerjee, R. V.; Johnston, N. L.; Sobeski, J. K.; Datta, P.; Matthews, R. G. *J. Biol. Chem.* **1989**, *264*, 13888–13895.

(19) Drummond, J. T.; Huang, S.; Blumenthal, R. M.; Matthews, R. G. *Biochemistry* **1993**, *32*, 9290–9295.

(20) Old, I. G.; Margarita, D.; Glass, R. E.; Saint Girons, I. *Gene* **1990**, *87*, 15–21.

(21) Smith, D. R. GenBank Accession No. U00017, 1994.

(22) Kaneko, T.; Tanaka, A.; Sato, S.; Kotani, H.; Sazuka, T.; Miyajima, N.; Sugiura, M.; Tabata, S. GenBank Accession No. D64002, 1995.

(23) Swinburne, J. *Nature* **1994**, *368*, 32–38.

(24) Chen, L. H.; Liu, M.-L.; Hwang, H.-Y.; Chen, L.-S.; Korenberg, J.; Shane, B. *J. Biol. Chem.* **1997**, *272*, 3628–3634.

(25) Leclerc, D.; Campeau, E.; Goyette, P.; Adjalla, C. E.; Christensen, B.; Ross, M.; Eydoux, P.; Rosenblatt, D. S.; Rozen, R.; Gravel, R. A. *Hum. Mol. Genet.* **1996**, *5*, 1867–1874.

(26) Li, Y. N.; Gulati, S.; Baker, P. J.; Brody, L. C.; Banerjee, R.; Kruger, W. D. *Hum. Mol. Genet.* **1996**, *5*, 1851–1858.

(27) White, O. GenBank Accession No. X92082, 1995.

(28) Vaupel, M. GenBank Accession No. X92082, 1995.

(29) Korch, C.; Mountain, H. A.; Wenzlau, J. M. Swiss Protein Accession No. P05694, 1995.

(30) Horton, R. M.; Ho, S. N.; Pullen, J. K.; Hunt, H. D.; Cai, Z.; Pease, L. R. *Methods Enzymol.* **1993**, *217*, 270–279.

(31) Numbering of nucleotides in the *methH* gene is based on the sequence deposited as GenBank Accession Number J04975 in which nt 223 is the first nucleotide in the coding sequence for the protein.

to nt 953–973 of the noncoding strand, again with changes introduced at nt 962 and 963. Two separate PCR reactions were carried out in a Perkin-Elmer DNA Thermal Cycler with Vent polymerase to minimize the possibility of errors in amplification. The first reaction contained primers A and B, and the second primers C and D. In both reactions the plasmid pCWG-05 which contains the truncated *metH* gene specifying the MetH(2-649) fragment was used as the template. The resulting products of amplification were isolated by agarose gel electrophoresis; the 360 and 510 bp bands were excised and purified with the GeneClean system. The purified products were then used as templates with primers A and D in a single PCR reaction. The product, 853 bp, was excised from an agarose gel and purified with the GeneClean kit. The PCR product was digested with *ApaI* and *BspEI* and the plasmid pCWG-05 was also digested with the same restriction enzymes. The PCR product was then ligated with T4 DNA ligase into pCWG-05 to yield plasmid pSH-01. The presence of the mutation was verified by DNA sequencing between *ApaI* (nt 974) and *BspEI* (nt 652) sites, using the Sequenase kit and primers A and D. The plasmid pHS01 was cut with *EcoRI* and *SacI*, and then the fragment containing the truncated *metH* gene was subcloned into the *EcoRI* and *SacI* sites of plasmid pCWG-02 and pMMA-07 to overexpress the Cys247 mutation in the MetH(2-649) fragment and the holoenzyme, respectively.

Expression and Purification of Wild-Type and Mutant Methionine Synthase Holoenzymes and Truncated MetH(2-649) Fragments.

The recombinant wild-type methionine synthase MetH(2-1227) from *Escherichia coli* K-12 strain XL1-Blue/pMMA-07³² was overproduced in metal-supplemented glucose minimal MOPS media (zinc chloride was added to a final concentration of 0.5 mM) and purified as described previously.³³ Truncated MetH(2-649) and the mutant proteins were overexpressed in zinc-supplemented Luria-Bertani medium (zinc chloride was added to a final concentration of 0.5 mM) and purified as previously described.¹¹

Metal Content Determination by ICP and Colorimetric Assay.

A sample of protein was prepared as previously described;⁷ the sample was washed three times with 10 mM Tris chloride buffer, pH 7.2, that had been scrubbed of metals by passage over Chelex 100 resin. The last wash filtrate was recovered and used as a blank. Samples were sent to the Garratt-Callahan Company (Millbrae, CA) to determine the metal content by ICP. Colorimetric assay for zinc with *p*-hydroxymethylmercuriphenylsulfonic acid and 4-(2-pyridylazo)resorcinol is detailed in an earlier paper.⁷

Assays. Methionine synthase specific activity was determined with a nonradioactive assay that measures the conversion of CH₃-H₄folate to H₄folate by derivitization of the latter to form CH⁺=H₄folate.³⁴ The assays utilizing exogenous cobalamin, the methyltetrahydrofolate-cob(I)alamin methyltransferase and methylcobalamin-homocysteine methyltransferase assays were described in a previous paper.¹¹

Stopped-Flow Studies of Turnover and Demethylation of Methylcobalamin MetH(2-1227) by Homocysteine. The holoenzyme and mutant protein were methylated as previously described.³⁵ The rate of demethylation of methylcobalamin holoenzyme by homocysteine was determined by stopped-flow spectroscopy at 25 °C under aerobic conditions, on a Hi-Tech instrument equipped with a tungsten lamp and a monochromator, with a photomultiplier tube operating at 580 V. Methylcobalamin enzyme (10 μM) in 50 mM Tris chloride buffer, pH 7.2, 100 mM KCl was reacted with homocysteine (100 μM) in 50 mM Tris chloride buffer, pH 7.2, 100 mM KCl. The formation of cob(I)-alamin was observed at 386 nm; the rate constant for demethylation of methylcobalamin holoenzyme was calculated from the initial rate of demethylation.

(32) *E. coli* strain XL1-Blue, in which our MetH proteins are expressed, contains a wild-type chromosomal copy of the *metH* gene, in addition to the overexpression plasmids. Thus crude extracts contain approximately 0.1% (relative to the plasmid-specified protein) wild-type MetH, which copurifies with the intact holoenzyme.

(33) Amaratunga, M.; Fluhr, K.; Jarrett, J. T.; Drennan, C. L.; Ludwig, M. L.; Matthews, R. G.; Scholten, J. D. *Biochemistry* **1996**, *35*, 2453–2463.

(34) Drummond, J. T.; Jarrett, J.; Gonzalez, J. C.; Huang, S.; Matthews, R. G. *Anal. Biochem.* **1995**, *228*, 323–329.

(35) Jarrett, J. T.; Goulding, C. W.; Fluhr, K.; Huang, S.; Matthews, R. G. *Methods Enzymol.* **1997**, *281*, 196–213.

XAS Sample Preparation. Wild-type MetE samples (3 mM) were equilibrated in 25 mM triethanolamine buffer containing 500 μM dithiothreitol. Sample I was treated with 4 equiv of CH₃-H₄PteGlu₃, as described by González et al.,⁶ to remove any bound homocysteine from the enzyme. Four equivalents of L-homocysteine were added to sample II. Wild-type MetH(2-649) protein (3 mM) was equilibrated in 10 mM Tris chloride buffer, pH 7.2. Sample II and sample III contained 12 mM L-homocysteine and D-homocysteine, respectively. Upon addition of substrate, the samples were immediately loaded into Lucite cuvettes (~150 μL) with 40 μm Kapton windows and rapidly frozen in liquid nitrogen.

XAS Measurements and Data Analysis. MetH(2-649) XAS data were collected at the National Synchrotron Light Source (NSLS) on beamline ×9B with a Si(220) double crystal monochromator and a Ni coated upstream mirror for harmonic rejection. The EXAFS spectra were measured by using 10 eV increments in the preedge region, 0.35 eV increments in the edge region, and 0.05 Å⁻¹ increments in the EXAFS region with integration times of 1 s in the preedge and edge and 1–20 s (*k*³ weighted) in the EXAFS for a total scan time of 40 min. All data were collected as fluorescence excitation spectra with a 13-element Ge solid-state detector array. The total integrated count rate was held below 40 kHz per channel to avoid saturation of the detector. The windowed Zn Kα fluorescence count rate was 0.8–1.0 kHz per channel in the EXAFS, giving a total of 2 × 10⁵ useful counts per scan at *k* = 13 Å⁻¹. The sample temperature was held at 25 K during data collection in a Displex cryostat.

XAS data were also collected on two independent preparations of MetE and a second preparation of MetH(2-649) at the Stanford Synchrotron Radiation Laboratory (SSRL). These data were measured on beamline VII-3, using a Si(220) double crystal monochromator detuned to 50% of the maximum intensity for harmonic rejection. The EXAFS were collected as fluorescence excitation spectra with a 13-element Ge solid-state detector array and measured in a manner similar to the first data set. The total integrated count rate was held below 90 kHz per channel, and the windowed count rate was 7–8 kHz per channel in the EXAFS region. The sample temperature was held at 10 K in an Oxford liquid helium flow cryostat during the measurements. For all samples, the initial and final spectra measured were compared to confirm the lack of radiation damage during the measurements.

Each detector channel of each scan was examined individually for glitches. All of the good channels (8 channels per scan) were averaged for each sample to give the final spectrum. Eight scans were then averaged for the MetH(2-649) and seven scans were averaged for the MetH(2-649) + homocysteine samples. The MetE data were treated as described previously.⁶ The X-ray energies were calibrated by collecting the absorption spectrum of a zinc foil reference at the same time as the fluorescence data, with the first inflection point of the zinc foil assigned as 9659 eV.

The XANES data were normalized by fitting the data both below and above the edge to tabulated X-ray absorption cross sections³⁶ with a single fourth order polynomial and a single scale factor.³⁷ The EXAFS background correction was performed by fitting a first-order polynomial to the preedge region, and a two-region cubic spline above the edge. The data were then converted to *k*-space using $k = (2m_e(E - E_0)/h^2)^{1/2}$, where $E_0 = 9675$ eV. Fourier transforms were calculated using *k*³ weighted data over a range of 2.0–12.8 Å⁻¹. The first shell ($R = 0.9–3.0$ Å for MetH(2-649); $R = 0.9–2.8$ Å for MetH(2-649) + L-homocysteine; and $R = 0.8–3.0$ Å for MetH(2-649) + D-homocysteine) was subsequently backtransformed over the same range. The resulting filtered data as well as the unfiltered EXAFS data were fit to eq 2 by using a nonlinear, least-squares algorithm. Filtered and unfiltered data gave equivalent structural parameters.

(36) McMaster, W. H.; Del Grande, N. K.; Mallett, J. H.; Hubbell, J. H. X-ray Absorption Cross Sections; U.S. Department of Commerce Report No. UCRL-50174-SEC 2-R1, 1969.

(37) Waldo, G. S. Ph.D. Thesis, University of Michigan, 1991.

$$\chi(k) = \sum_i \frac{N_i S_i(k) A_s(k)}{k R_i^2} \exp(-2k^2 \sigma_i^2) \exp\left(\frac{-2R_i}{\lambda}\right) \sin(2kR_i + \phi_i(k)) \quad (2)$$

EXAFS data are described by eq 2, where $\chi(k)$ is the fractional modulation in the absorption coefficient above the edge, N_s is the number of scatterers at a distance R_{as} , $A_s(k)$ is the effective backscattering amplitude, σ_{as}^2 is the root-mean-square variation in R_{as} , $\phi_{as}(k)$ is the phase shift experienced by the photoelectron wave in passing through the potentials of the absorbing and backscattering atoms, $S_i(k)$ is a scale factor specific to the absorber–scatterer pair, and the sum is taken over all scattering interactions.³⁸ The program FEFF version 6.01^{39,40} was used to calculate amplitude and phase functions, $A_s(k) \exp(-2R_{as}/\lambda)$ and $\phi_{as}(k)$, for a zinc–oxygen interaction at 2.00 Å, a zinc–nitrogen interaction at 2.05 Å, and a zinc–sulfur interaction at 2.30 Å. The scale factors, $S_S(k) = 1.02$ and $S_{N/O}(k) = 0.85$, and the shift in E_0 relative to 9675 eV, $\Delta E_0 = 9$ eV, were calibrated by fitting the EXAFS data for crystallographically characterized zinc models.⁵

The individual fits were performed allowing R and σ to vary for each shell while holding all other parameters fixed. Accurate quantitation of S and N/O ligation is difficult due to the destructive interference between Zn–S and Zn–(N/O) EXAFS. As described by Clark-Baldwin et al.,⁵ fits were performed with the total zinc coordination number fixed at four while the number of nitrogen and sulfur ligands is varied in increments of 0.25. For each fit, the percent improvement relative to a two-shell 2S + 2S fit, P_i , was calculated (eq 3) as a function of percent S. In eq 3, \mathcal{G}_i is the root-mean-square deviation in the i th N + S fit ($n_i N + (4 - n_i)S$), \mathcal{G}_{2S+2S} the root-mean-square-deviation for the 2S + 2S fit, and \mathcal{G}_{4S} the root-mean-square deviation for the one-shell, 4S fit.⁵ The dependence of P_i and σ_s^2 on percent S can be used to distinguish between ZnS₄, ZnS₃N, and ZnS₂N₂ sites. In model studies, this approach provides reliable discrimination between these sites.⁵

$$P_i = \frac{\mathcal{G}_{2S+2S} - \mathcal{G}_i}{\mathcal{G}_{4S}} (100\%) \quad (3)$$

Results

Native Zinc Environments. The k^3 -weighted, background subtracted zinc EXAFS data for MetH(2-649) and MetE (see Figure S1 in Supporting Information) are very similar, although the oscillations in the MetH(2-649) spectrum have a larger amplitude and slightly higher frequency than those in the MetE EXAFS. This difference can be seen more clearly in the Fourier transforms of the spectra (Figure 1). The main peak in the Fourier transform of the MetH(2-649) EXAFS data is almost twice the height of that for the MetE data. In addition, the MetH peak is noticeably narrower than that for MetE. These observations suggest that the zinc site in MetH has a larger fraction of longer-distance, high molecular weight (e.g., sulfur) ligands and a smaller fraction of shorter-distance, low molecular weight (e.g., O/N) ligands in comparison with MetE.

Neither data set could be well modeled with a single shell of scatterers (Table 1). As described previously, the EXAFS data for MetE were best modeled with a shell of 2(N/O) ligands at ~ 2.03 Å and a shell of 2S ligands at 2.31 Å.⁶ In contrast, the EXAFS data for MetH(2-649) were best modeled with a shell of one low-Z (N/O) ligand at ~ 2.14 Å and a shell of 3S ligands

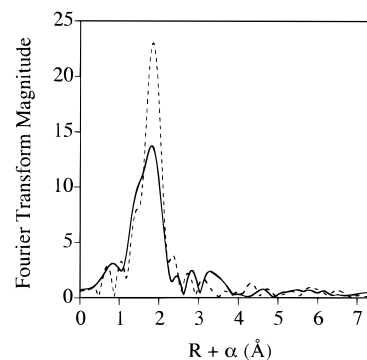


Figure 1. Fourier transforms of the native methionine synthase EXAFS spectra: solid line, MetE; dashed line, MetH(2-649).

Table 1.^a EXAFS Fitting Results for Methionine Synthase Enzymes

sample	S			N/O			\mathcal{G}'^b
	<i>N</i>	<i>R</i> (Å)	σ^2 (10^3 Å ²)	<i>N</i>	<i>R</i> (Å)	σ^2 (10^3 Å ²)	
MetE	4	2.30	8.7				0.042
	2	2.31	3.4	2 N	2.04	3.8	0.015
	2	2.31	3.4	2 O	2.02	5.9	0.013
MetE + L-homocysteine	4	2.33	5.8				0.026
	3	2.33	3.6	1 N	2.07	2.3	0.016
	3	2.33	3.8	1 O	2.05	4.4	0.016
MetH(2-649)	4	2.32	4.7				0.049
	3	2.32	3.9	1 N	2.15	8.8	0.031
	3	2.32	3.2	1 O	2.12	10.7	0.030
MetH(2-649) L-homocysteine	4	2.35	3.8				0.018
	3	2.36	2.4	1 N	2.16	1.9	0.017
	3	2.36	2.4	1 O	2.13	4.7	0.019
MetH(2-649) D-homocysteine	4	2.33	4.8				0.031
	3	2.33	3.6	1 N	2.16	3.1	0.015
	3	2.33	3.6	1 O	2.14	4.4	0.015

^a Results for fits to filtered data. Similar parameters were obtained for fits to unfiltered data but with higher \mathcal{G}' values due to the neglect of outer shell scattering. On the basis of the reproducibility of the data and the dependence of fit results on filter parameters, the estimated precision is 0.03 Å in $R_{N/O}$ and 0.02 Å in R_S . Uncertainty in σ^2 is ca. 2×10^{-3} Å². ^b $\mathcal{G}' = \{[k^6(\text{data} - \text{fit})^2]/N\}/(N_{\text{idp}} - N_{\text{var}})$ where N is the number of data points, $N_{\text{idp}} = (2\Delta k \Delta R)/\pi$ is the number of independent data points, and N_{var} is the number of variable fitting parameters.

at 2.32 Å. These calculated bond distances are similar to those found in 4-coordinate zinc model complexes with comparable first-shell ligation.^{41,42} Bond-valence-sum calculations⁴³ confirm a coordination number of four, and are inconsistent with coordination numbers of 3 and 5. The sulfur atoms seen by EXAFS most likely come from cysteine amino acid residues. The low-Z contribution could be either exogenous (H₂O or phosphate) or endogenous (His or carboxylate). Although there are weak outer-shell scattering features in the Fourier transforms of the MetE EXAFS that could be attributed to imidazole scattering, it is difficult to establish unambiguously that these are due to imidazole.⁵

Effects of the Mutation of Cys247Ala in Meth Holoenzyme and MetH(2-649) Protein. Since the EXAFS spectra for the MetH(2-649) protein were best modeled with three sulfur ligands coordinating the zinc, mutagenesis studies were performed to ascertain if the third conserved cysteine, Cys247, could also be a candidate zinc ligand. The Cys247Ala mutation was incorporated into the wild-type MetH (MetH2-1227) and into the 71 kDa fragment containing the substrate binding regions (MetH2-649), and the corresponding proteins were overexpressed and purified to homogeneity. The zinc content of Cys247Ala MetH(2-1227) was 0.15 mol equiv of zinc per mol of protein, while the Cys247Ala MetH(2-649) contained 0.09 mol equiv of zinc per mol of protein. Despite the retention

(38) Teo, B. K. *EXAFS: Basic Principles and Data Analysis*; Springer-Verlag: New York, 1986.

(39) Rehr, J. J.; Mustre, D. L. J.; Zabinsky, S. I.; Albers, R. C. *J. Am. Chem. Soc.* **1991**, *113*, 5135–5140.

(40) Rehr, J. J.; Albers, R. C.; Zabinsky, S. I. *Phys. Rev. Lett.* **1992**, *69*, 3397–3400.

(41) Corwin, D. T., Jr.; Koch, S. A. *Inorg. Chem.* **1988**, *27*, 493–496.

(42) Gruff, E. S.; Koch, S. A. *J. Am. Chem. Soc.* **1989**, *111*, 8762–8763.

(43) Brown, I. D.; Altermatt, D. *Acta Crystallogr.* **1985**, *B41*, 244–247.

Table 2. Specific Activities of Wild-Type and Mutant MetH Proteins and Their Zinc Content after Isolation from Cells Grown in Metal-Unsupplemented Medium

form of MetH	specific activity ($\mu\text{mol min}^{-1} \text{mg}^{-1}$)	Zn per mol of protein
wild-type	10.94	0.76 ^c
Cys310Ala	0.011 ^{a,b}	0.01
Cys310Ser	0.018 ^{a,b}	0.05 ^c
Cys311Ala	0.014 ^{a,b}	0.02
Cys311Ser	0.021 ^{a,b}	0.06 ^c
Cys247Ala	0.018 ^a	0.15

^a Strain XL1-Blue, in which our MetH proteins are expressed, contains a wild-type chromosomal copy of the metH gene, in addition to the overexpression plasmids. Thus, crude extracts contain approximately 0.1% wild-type MetH (relative to the plasmid-specified protein), which copurifies with the desired mutant enzymes and accounts for the low residual activity. ^b Data published in ref 7. ^c Data published in ref 11.

Table 3. Comparison of the Second-Order Rate Constants for Reaction of Wild-Type MetH(2-649) and Mutant Proteins with Exogenous Cobalamin and Their Zinc Contents

form of MetH(2-649)	Zn per mol of protein	cob(I)alamin + $\text{CH}_3\text{-H}_4\text{folate}$ ($\text{M}^{-1} \text{s}^{-1}$)	methylcobalamin + Hcy ($\text{M}^{-1} \text{s}^{-1}$)
wild-type	0.82 ^a	594 ^b	2320 ^b
Cys247Ala	0.09	589 ^b	<10
Cys310Ala	0.02 ^a	593 ^b	<10 ^b
Cys311Ala	0.03 ^a	590 ^b	<10 ^b

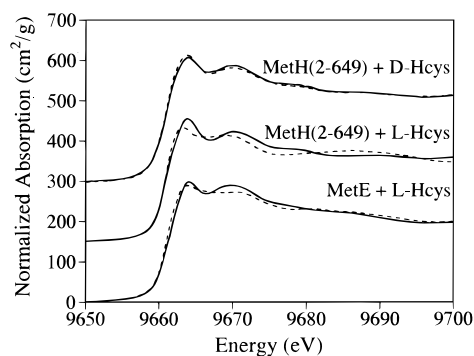
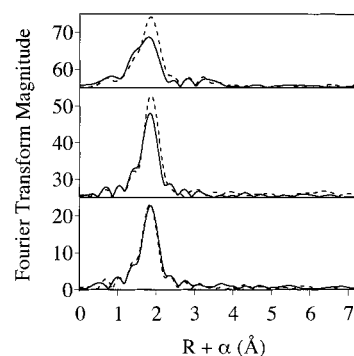
^a Data published in ref 11 and obtained after isolation of MetH from cells grown in zinc-supplemented media. ^b Data published in ref 7.

of some zinc binding activity, mutation of Cys247 to alanine rendered the mutant holoenzyme catalytically inactive as compared to wild-type MetH holoenzyme (Table 2). The low level of zinc binding in Cys247Ala MetH(2-1227) is consistent with the properties conferred by the Cys310Ala and Cys311Ala mutants, which contained <0.06 mol equiv of zinc per mol of protein.⁷

To monitor the effect of the Cys247Ala mutation on the binding and activation of homocysteine and methyltetrahydrofolate, studies involving catalysis of the methyl transfer from exogenous methylcobalamin to homocysteine were performed with Cys247Ala MetH(2-649) mutant protein. Although this mutant protein had no methylcobalamin-homocysteine methyltransferase activity, it retained the ability to catalyze the methyl transfer from methyltetrahydrofolate to cob(I)alamin with a second-order rate constant that was the same as that for the wild-type MetH(2-649) protein (Table 3). Hence, the residue Cys247 is required for homocysteine binding and activation, as are residues Cys310 and Cys311.¹¹

Demethylation of the wild-type methylcobalamin form of MetH(2-1227) by homocysteine was followed by observing the formation of cob(I)alamin at 386 nm, under aerobic conditions (Figure S2). As previously reported,⁷ the rate constant for the demethylation of wild-type methylcobalamin MetH(2-1227) by homocysteine is 10.9 s^{-1} in Tris chloride buffer, pH 7.2. We observed no demethylation of the Cys247Ala MetH(2-1227) mutant. This observation is in agreement with the lack of activity observed for this mutant and with the failure of the Cys310Ser and Cys311Ser MetH(2-1227) mutant proteins to be demethylated by homocysteine.⁷

The Effect of Homocysteine on Zinc Site Structure. To determine whether the zinc ion in methionine synthase enzymes is directly involved in the binding of homocysteine, XANES and EXAFS spectra were measured for MetE, MetH, and MetH(2-649) both with and without added homocysteine (Figure 2,

**Figure 2.** Normalized XANES spectra of native methionine synthase enzymes (solid lines) and enzymes + D- or L-homocysteine (dashed lines): (top) MetH(2-649) with and without D-homocysteine; (middle) MetH(2-649) with and without L-homocysteine; and (bottom) MetE with and without L-homocysteine. XANES spectra of the MetH holoenzyme with and without L-homocysteine (not shown) are identical to the spectra measured for MetH(2-649). The spectra are plotted on the same scale, offset vertically for clarity.**Figure 3.** Fourier transforms of EXAFS data for native methionine synthase enzymes with and without homocysteine (Hcy) (solid = MetE or MetH alone; dash = enzyme + Hcy): (top) MetE and MetE + L-Hcy; (middle) MetH(2-649) and MetH(2-649) + L-Hcy; and (bottom) MetH(2-649) and MetH(2-649) + D-Hcy. All spectra are plotted on the same scale, offset vertically for clarity.

bottom pairs of spectra). The zinc XANES spectra for both of the wild-type enzymes show distinct edge transitions at ~ 9663 and ~ 9670 eV. For both enzymes, addition of homocysteine resulted in a decrease in intensity and a shift to lower energy for the ~ 9663 eV transition. The higher energy transition became much weaker and less well resolved. XANES measurements of ZnS_2N_2 , ZnS_3N , and ZnS_4 model compounds⁵ described in the accompanying paper showed a similar trend as nitrogen ligands were exchanged for sulfur ligands.

To determine if the changes observed in the XANES are specific to L-homocysteine, XANES spectra were measured on a sample of MetH(2-649) + D-homocysteine (Figure 2, top spectra). Although there are minor variations in the XANES spectra for MetH(2-649) + D-homocysteine and native MetH(2-649) (slightly larger intensity at ~ 9663 eV and slightly lower intensity at ~ 9670 eV), the overall XANES appearance of the spectrum for MetH(2-649) changes very little when D-homocysteine is added.

The EXAFS spectra of the methionine synthase enzymes with and without added homocysteine are shown in the Supporting Information (Figure S3) and the corresponding Fourier transformed spectra in Figure 3. The increase in Fourier transform amplitude on addition of L-homocysteine to either enzyme is similar to the differences between the native MetE and MetH(2-649). As was seen in the XANES, D-homocysteine has no significant effect on the EXAFS spectra. Qualitatively, both

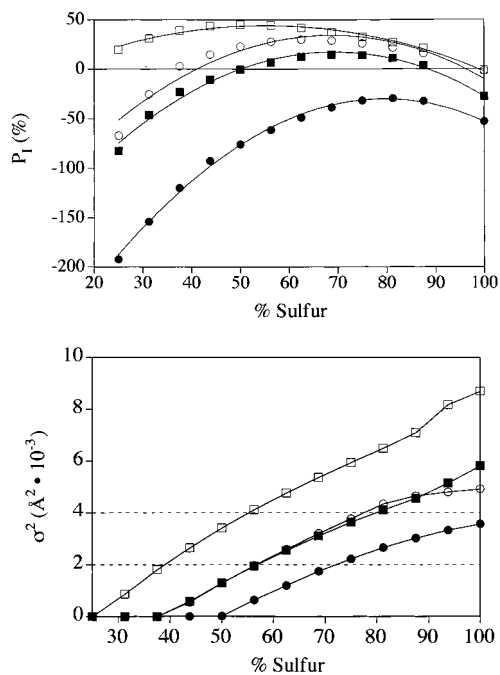


Figure 4. Fit statistics as a function of the percent sulfur used in the fit for MetE (squares) and MetH(2-649) (circles). Open symbols are the native enzymes, closed symbols are enzyme + homocysteine (Hcy). (A) P_1 plotted vs percent S. The native MetE curve has a maximum at ~50% sulfur; MetE + L-Hcy and the native MetH(2-649) have maxima at 60–70% sulfur; MetH(2-649) + L-Hcy has a maximum at ~80% sulfur. In model compounds, these maxima are typical of ZnS_2N_2 , ZnS_3N , and ZnS_4 ligation, respectively.⁵ The negative P_1 values for MetH(2-649) + L-Hcy reflect the fact that all of the S + N fits are worse than two shell, 2S + 2S fits, as observed in authentic ZnS_4 models. (B) σ_s^2 vs percent S. In model studies, fits using the correct S:N ratio give $\sigma_s^2 = 2-4 \times 10^{-3} \text{\AA}^2$ (shown by horizontal dashed lines) supporting the assignments in part A).

the EXAFS and the XANES suggest that the addition of L-homocysteine to either MetE and MetH(2-649) results in replacement of a low-Z with a sulfur atom.

Quantitative analysis supports these conclusions. For MetE, the maximum in the P_1 vs percent S curve occurs at about 50% S, and the observation of $\sigma_s^2 = (2-4) \times 10^{-3} \text{\AA}^2$ at 50% S are all typical of the behavior of ZnS_2N_2 sites.⁵ Similarly, the dependence of P_1 and σ_s^2 on percent S for MetE + L-homocysteine and MetH(2-649) are typical of the behavior of ZnS_3N sites. The similarity of the curve fitting for these sites, as illustrated by Figure 4, demonstrates that they have the same ligation, despite the minor differences in their XANES spectra and the Fourier transforms of their EXAFS spectra. Finally, the fitting behavior for MetH(2-649) + L-homocysteine, in particular the negative P_1 values and the unrealistically low σ_s^2 values for 75% S fits, indicates that this sample has a ZnS_4 site. Negative P_1 values, which indicate that the S + N fits are worse than two-shell S + S fits, are characteristic of attempts to fit ZnS_4 data to an S + N model.⁵ Determination of absolute coordination number by EXAFS is difficult. However, the similarity of the average Zn–S bond lengths for all five samples (Table 1) suggests that all of the Zn sites are four coordinate. Bond-valence-sum calculations support this conclusion.

Discussion

The work presented here demonstrates the power of the EXAFS fitting technique described in the accompanying paper⁵ to characterize zinc in metalloenzymes. Both methionine

synthase enzymes studied in this work exhibit four-coordinate ligation of zinc, but they do not have identical ligands. Best fits were obtained assuming 2(N/O) + 2S ligands for MetE and 1(N/O) + 3S ligands for MetH(2-649). Previous work had identified two cysteines, Cys310 and Cys311, as candidate ligands for the zinc in MetH,⁷ and the mutational analysis described in this paper is consistent with Cys247 providing a third amino acid ligand to the zinc in the MetH.

The zinc site in MetH shows no obvious similarity with zinc sites described in other enzymes, but vicinal cysteines are involved in ligation of tetrahedrally coordinated zinc in the four metal clusters of metallothionein.⁴⁴ The GGC³¹⁰C³¹¹G motif in MetH is conserved in betaine-homocysteine methyltransferase,⁴⁵ suggesting that this enzyme will also employ zinc for homocysteine binding and activation.

Only one of the candidate ligands for zinc in MetE, Cys726, has been identified. However, the finding that the protein contributes one additional cysteine and one low-Z ligand suggests the conserved His⁶⁴¹-Met-Cys⁶⁴³ motif as a candidate for providing additional ligands. This motif appears also in the sequences of two related methyltransferase isozymes that catalyze methyl transfer from methylcobamide to coenzyme M (ethanethiol-sulfonate), and has been implicated in the binding of zinc to those methyltransferases.⁴⁶

Compelling evidence was also obtained for the direct involvement of zinc in the activation of the thiol substrates of the two forms of methionine synthase. Addition of homocysteine resulted in replacement of an O/N ligand by a S in each case. These results illustrate the sensitivity of the EXAFS analysis to the number of low-Z ligands. Although the zinc ligation is different in the two enzymes, addition of L-homocysteine to either MetE or MetH caused a similar change in the XANES spectra. The Zn site appears to remain 4-coordinate in both cases, suggesting that the new sulfur ligand, presumably the L-homocysteine thiol, displaces a low-Z ligand when it binds to either enzyme.

The observation that the MetE site contains only two cysteine ligands is interesting in the context of the model studies of Wilker and Lippard,^{3,47} which suggest that activation of thiols coordinated to zinc requires a highly dissociative zinc complex with a net charge of -2 . Although EXAFS cannot be used to identify the low-Z ligand in MetE, it is possible that the zinc site in the substrate-bound form of MetE is coordinated to two cysteines and a histidine from the protein, along with the sulfur of the homocysteine substrate. Based on model studies, such a site should be substantially less reactive than the corresponding MetH complex. A curious property of the MetE enzyme is the requirement for phosphate for maximal catalytic activity.¹⁴ Studies are now in progress to test the hypothesis that the phosphate ion is required for conversion of the relatively unreactive 4-coordinate MetE zinc complex to a much more reactive 5-coordinate complex with the phosphate anion as an additional ligand. A possible mechanism, consistent with the present data and with the hypothesized role of phosphate, is shown in Figure 5.

The role of zinc may be to stabilize the homocysteine thiolate at neutral pH, thus activating the thiol for methyl transfer under physiological conditions in both methionine synthase enzymes.

(44) Robbins, A. H.; McRee, D. E.; Williamson, M.; Collett, S. A.; Xuong, N. H.; Furey, W. F.; Want, B. C.; Stout, C. D. *J. Mol. Biol.* **1991**, *221*, 1269–1293.

(45) Garrow, T. A. *J. Biol. Chem.* **1996**, *271*, 22831–22838.

(46) LeClerc, G. M.; Grahame, D. A. *J. Biol. Chem.* **1996**, *271*, 18725–18731.

(47) Wilker, J. J.; Lippard, S. J. *J. Am. Chem. Soc.* **1995**, *117*, 8682–8683.

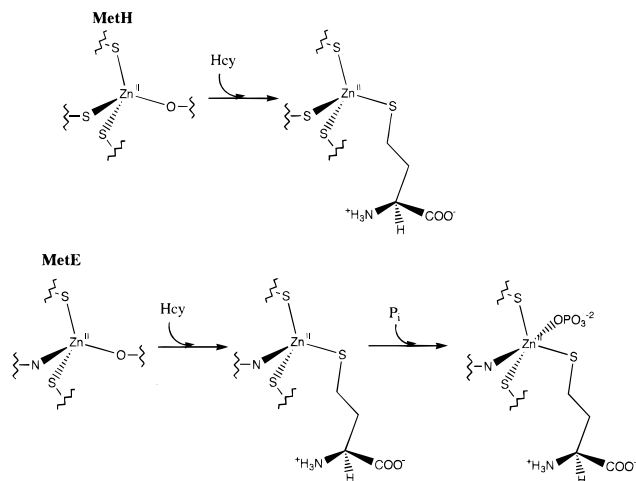


Figure 5. Possible mechanisms for MetH and MetE. MetH binds homocysteine to form a 4-coordinate zinc tetrathiolate complex. The ligand in the substrate free complex has not been identified, but is thought to be a low-Z ligand. MetE binds homocysteine to form a 4-coordinate trithiolate complex. Although not definitely established, the fourth ligand is probably a histidine, and the complex therefore has a net charge of -1 . On the basis of model studies, such complexes are expected to be much less reactive than the corresponding complexes with a net charge of -2 . We postulate that addition of phosphate, which is required for maximal catalytic activity, results in an expansion of the coordination sphere, giving a net charge of -2 and thereby enhancing the reactivity of homocysteine by increasing the dissociative character of the complex.

A precedent for zinc acting as a catalyst in the nucleophilic attack of a thiolate on a methyl group is found in the Ada protein of *E. coli*.⁴ NMR studies of ¹¹³Cd-substituted Ada protein with ¹³C-labeled CH₃I⁴⁸ and methylated DNA⁴⁹ have shown that the methyl group is transferred to the thiolate of the Cys69 zinc ligand. Related kinetic studies involving [Zn(SC₆H₅)₄]²⁻ models and (CH₃O)₃PO have shown that highly dissociative zinc tetrathiolate complexes can serve to provide a reservoir of reactive free thiolate at neutral pH.^{3,47} Recently, in rat farnesyl transferase (FTase), a zinc cofactor has been implicated in the binding of a cysteine residue of protein substrates, such as Ras proteins, orienting, and perhaps activating, the cysteine for transfer of the farnesyl group from farnesyl pyrophosphate (FPP). Huang et al.⁵⁰ were able to show that, upon addition of FPP and peptide substrate to a Co²⁺-substituted form of FTase, the extinction coefficient for the Co–S ligand-to-metal charge-transfer transition increased in a manner consistent with additional cobalt–sulfur coordination, presumably by the cysteine thiolate of the peptide. Since the crystal structure of rat FTase shows the zinc to be pentacoordinate with a water molecule filling one of the coordination sites,⁵¹ a mechanism involving the displacement of a water ligand by the thiol of the substrate would be compatible with the changes observed in farnesyl transferase. A similar mechanism is possible for both forms of *E. coli* methionine synthase, although the identity of the displaced low-Z ligand is not clear in either enzyme.

(48) Myers, L. C.; Wagner, G.; Verdine, G. L. *J. Am. Chem. Soc.* **1995**, *117*, 10749–10750.

(49) Ohkubo, T.; Sakashita, H.; Sakuma, T.; Kainosho, M.; Sekiguchi, M.; Morikawa, K. *J. Am. Chem. Soc.* **1994**, *116*, 6035–6036.

(50) Huang, C.-C.; Casey, P. J.; Fierke, C. A. *J. Biol. Chem.* **1997**, *272*, 20–23.

(51) Park, H.-W.; Boduluri, S. R.; Moomaw, J. F.; Casey, P. J.; Beese, L. S. *Science* **1997**, *275*, 1800–1804.

(52) Goulding, C. W.; Matthews, R. G. Unpublished data.

(53) Myers, L. C.; Jackow, F.; Verdine, G. L. *J. Biol. Chem.* **1995**, *270*, 6664–6670.

(54) Sauer, K.; Thauer, R. K. *Eur. J. Biochem.* **1997**, *249*, 280–285.

Both the XANES and the EXAFS spectra indicate that there are few if any changes in the zinc binding site of MetH(2-649) when D-homocysteine is added. Although the binding constant of D-homocysteine to MetH is not known, the absence of change in the XANES and EXAFS is an important control, demonstrating that addition of thiol alone is not sufficient to cause a change in the Zn site. This demonstrates that the homocysteine binding site is not defined solely by the Zn–S(homocysteine) interaction. There may be, for example, electrostatic interactions between the protein and the amine and carboxylate portions of homocysteine. These interactions would provide additional binding energy, helping to anchor the homocysteine in the appropriate geometry. In such a structure, the thiolate side chain of the incorrect D-enantiomer would not be oriented appropriately to bind to the zinc. Since L-alanine does not block L-homocysteine binding in MetH(2-649),⁵² it is unlikely that the putative electrostatic interaction is strong in comparison with the Zn–S interaction. Nevertheless, this may provide a portion of the enzyme–substrate interaction energy. These observations would explain the absence of inhibition by simple alkylthiolates.

It is intriguing that the changes in the XANES spectra seen on addition of substrate are quite similar for the two isozymes, despite the presence of different Zn ligation. These changes may arise, at least in part, from replacement of a low-Z ligand with a thiolate ligand. However, we have noted previously the sensitivity of Zn XANES spectra to small variations in geometry.⁵ It is possible that the XANES difference seen in Figure 2 reflects, at least in part, geometric rather than ligation changes. For example, the substrate-free and substrate-bound forms may differ in their distortions from tetrahedral symmetry. If so, changes in the sulfur–sulfur multiple scattering could account for the changes in the XANES. In this case, the similarity in the changes induced by L-homocysteine may be a reflection of similar, substrate-induced changes in the geometry of the Zn site. We are currently examining the extent to which similar spectral changes are seen in model compounds and in related zinc enzymes.

A role for zinc in enzyme-catalyzed methyl transfers to sulfur is an emerging theme in bioinorganic chemistry,² with strong evidence of a role for zinc in MetE, MetH, and the Ada protein.^{6,7,53} Zinc has also been found in two methyltransferase isozymes from *Methanosarcina barkerii* that catalyze methyl transfer from methylcobamide to coenzyme M (ethanethiol sulfonate),⁴⁶ and incubation of these enzymes with EDTA has been shown to result in loss of activity. Very recent studies have demonstrated that the zinc ion in the Mt2A methylcobamide:coenzyme M methyl transferase isozyme is essential for catalytic activity.⁵⁴ EXAFS spectroscopy is a powerful tool for probing the ligand environment of the zinc in these enzymes.

Acknowledgment. This work was supported in part by grants from the NIH (GM-38047 to J.P.H. and GM24908 to R.G.M.). SSRL and NSLS are supported by the US Department of Energy with additional support from the NIH Research Resource program.

Supporting Information Available: Figures showing the measured EXAFS spectra and best fits (Figures S1 and S3) and stopped-flow trace showing formation of cob(I)alamin from methylcobalamin and L-homocysteine (Figure S2) (3 pages, print/PDF). See any current masthead page for ordering information and Web access instructions.